RESEARCH ON NDVI NORMALIZATION METHOD BASED ON GF IMAGES

Yuting Tao[1], Wenli Huang[1*], Wenxia Gan[2], Huanfeng Shen[1]

[1]School of Resource and Environmental Sciences, Wuhan University, Wuhan, Hubei, 430079, PR China
[2]School of Civil Engineering and Architecture, Wuhan Institute of Technology

Commission III, WG III/6

KEY WORDS: NDVI products, GF-1, GF-2, Single-scene Global Linear Model, Multi-scene Global Linear Model, Maximum Value Composite

ABSTRACT:

The existing NDVI products have problems in terms of low spatial resolution and inconsistent values at a large geographical scale. Based on medium and high-resolution multi-source remote sensing data (GF-1 and GF-2 data), this paper normalized NDVI by combining absolute radiation normalization with relative radiation normalization. And the existing relative radiation normalization method, single-scene global linear normalization (SGloLM) method, is improved to adapt to the production of large-range high-resolution NDVI products. Aiming at the problem of obvious mosaic seams when the SGloLM method is applied to multi-scene images, it is mainly improved from two aspects. One is to improve the coefficient solution of the SGloLM algorithm and propose a new method considering the surrounding multi-scene data, the multi-scene global linear model (MGloLM). The other is to incorporate the Maximum Value Composite (MVC) method to synthesize the maximum value of NDVI at different times in a season, to represent the optimal situation of vegetation growth in the current season. In this study, combined experiments of different methods were performed, as well as qualitative and quantitative evaluations. The experimental results show that SGloLM+MVC and the MGloLM+MVC methods can better eliminate the mosaic seams, and their histogram is most similar to the histogram of standard data, and all quantitative evaluation indexes of SGloLM+MVC are optimal (CC=0.7804, MAD=0.0643, RMSE=0.1012).

1. INTRODUCTION

Vegetation plays a vital role in the ecosystem and is closely related to natural environment elements such as soil, topography, climate, and hydrology, and has a profound impact on the energy balance of the earth-atmosphere system (Zhang, 2009), and has long been of great interest to scientists and governments worldwide. As one of the most effective means of global vegetation monitoring at present, satellite remote sensing can be free from the constraints of social and natural conditions. And it can quickly obtain large-scale observation data, which provides us with conditions for studying and monitoring global or regional vegetation growth changes (Guo, 2003). Based on the vegetation's spectral properties, various vegetation indexes have been generated by linear or nonlinear combination operations on the visible light and near-infrared bands of remote sensing data (Guo, 2003; Zhang, 2009). So far, more than one hundred and fifty vegetation index models have been proposed in various literature. Among them, the Normalized Difference Vegetation Index (NDVI) proposed by Deering (1978) is not only easy to calculate, but also enhances the sensitivity to vegetation by eliminating most of the effects related to sensor radiometric calibration, topography, atmospheric conditions, and observation angle (Ge, 2016). Hence, it has become one of the most widely used vegetation indexes today. As one of the important parameters to describe the characteristics of surface vegetation coverage, vegetation index is a simple, effective and empirical measure of surface vegetation status (Guo, 2003). It has been widely used in qualitative and quantitative evaluation of vegetation coverage and its growing status. The NDVI obtained based on satellite remote sensing data can comprehensively reflect the growth status and seasonal variation characteristics of vegetation, and provide important support for the dynamic monitoring of vegetation at the regional and global scales. At present, it has been widely used in the fields of vegetation growth monitoring, seasonal and interannual variation analysis, etc (Gan, 2015).

However, most of the existing vegetation index products use single remote sensing data, which have certain deficiencies in temporal resolution, spatial resolution, accuracy and stability (Ge, 2016), and the integrated use of multi-source remote sensing data can compensate for these deficiencies to a certain extent. Because of the differences in sensors and imaging conditions of multi-source remote sensing data, it is necessary to normalize them. Radiation normalization is divided into absolute radiation normalization and relative radiation normalization, and when normalizing multi-temporal data from a single sensor, simple relative radiation normalization can achieve high accuracy. However, in quantitative applications, the absolute radiation normalization should be combined with the relative radiation normalization, and the influence of reflection differences caused by different sensors due to spectral response characteristics and atmospheric correction on the normalization results should be considered. And the normalization of multi-source data should be carried out at the surface reflectance level to truly achieve normalization between different images from different sensors (Xu, 2019). For a long time, many research scholars have conducted a lot of research work on the normalization of multi-source remote sensing data. However, the previous studies on NDVI normalization of multi-source data mostly focus on low and medium-resolution data such as MODIS and Landsat, and less on high-resolution data.

*Corresponding author. Email: wenli.huang@whu.edu.cn (Wenli Huang).

This study proposes an improved normalization method for the construction of high-resolution quantitative product datasets to improve the dynamic monitoring of urban vegetation resources by normalizing medium and high-resolution multi-source remote sensing data based on previous experiences and methods.

2. MATERIALS AND METHODS

2.1 Data and study area

This study used DN data from the GaoFen-1 (GF-1) wide field of view (WFV) sensor and the GF-2 panchromatic multispectral sensor (PMS). These data were available for free download from the China High-resolution Earth Observation System (CHEOS) grid platform (www.cheosgrid.org.cn). The GF-1 satellite carries a 16 m-resolution WFV multispectral camera with an imaging width of 800 km and a temporal resolution of 4 days. The GF-2 satellite has a multispectral resolution of 4 m, an imaging width of 45 km (Wu, 2014), and an absolute temporal resolution of 69 days. Both of these multispectral cameras have four bands, and in this study, band 3 (red band) and band 4 (near-infrared band) were used. The spectral response function curves of GF-1 WFV data and GF-2 PMS data are shown in Figure 1 (GF-1 WFV1 and GF-2 PMS2 as an example). It can be seen from the figure that the spectral response function curves of the two are very similar, which is the basic condition for the relative radiation normalization of the GF-2 PMS data with the GF-1 WFV data as the reference data.

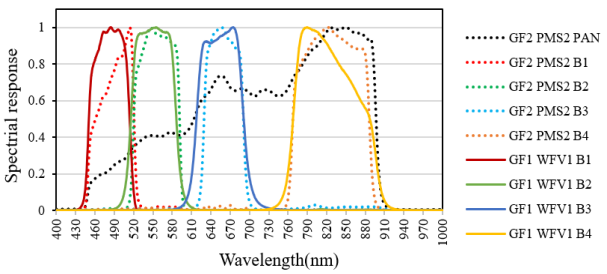

Figure 1. Spectral response function curves of GF-1 WFV and GF-2 PMS.

The GF-1 WFV data and GF-2 data used in the experiments are located in Wuhan, Hubei Province. Wuhan is the central city in the central region of China, located in the eastern part of the Jianghan Plain and the middle reaches of the Yangtze River. The specific geographical location is from 113 °41' to 115 °05' E and 29 °58' to 31 °22' N. Wuhan is the central city of the national synthesis coordinated reforms experimental plot of "two types society", which is resource-saving and environment-friendly, and pays attention to forestry ecological construction and resource protection. The typical vegetation in Wuhan is a mixed forest consisting of subtropical evergreen broadleaf forest and deciduous broadleaf forest. Details about the data were shown in Figure 2 and Table 1.

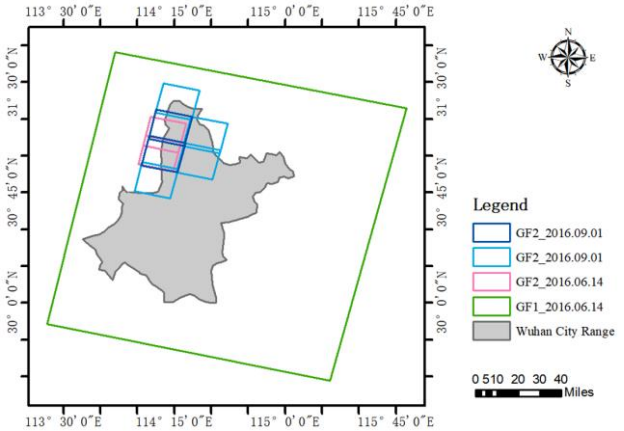

Figure 2. GF-1 and GF-2 data coverage maps used in the study.

Sensor	Scene ID	Acquisition Data	Pixel Size (m)
GF-1 WFV3	2510476	14/06/2016	16
GF-2 PMS1/2	2509145, 2509146	14/06/2016	4
	2763984, 2763985, 2763983, 2764226, 2764227, 2763986	01/09/2016	4

Table 1. GF-1 and GF-2 data used in the study.

2.2 Data pre-processing

In this study, absolute and relative radiation normalization were combined. The high-resolution NDVI data to be normalized were first calculated from surface reflectance data. In addition, the normalization process requires correspondingly medium-resolution reference, classification, and cloud mask data.

The pre-processing of GF-1 and GF-2 data mainly includes the following steps:

Step 1. Orthorectification: It is the process of correcting geometric distortions caused by sensors, terrain and other factors by using ground control points and certain mathematical models. Here the orthorectification of the image is realized by using the rational polynomial coefficients (RPC) files that come with the image and the Digital Elevation Model (DEM) that comes with the ENVI software. The RPC file of the high-resolution remote sensing image is a transformation matrix solved from the orbital parameters of the sensor and some other physical parameters, combined with ground control points (Zhuo, 2017).

Step 2. Radiation calibration: It is the process of converting the original dimensionless brightness gray value (DN value) recorded by the sensor into the absolute radiance value with actual physical significance. This process can eliminate the errors caused by the sensor, to determine the exact radiation value of the sensor at the entrance.GF-1 and GF-2 satellite sensor radiation calibration formula is as follows:

$$L_c(\lambda_c) = gain \cdot DN + offset \quad (1)$$

where $L_c(\lambda_c)$ = a band radiation luminance value
$gain$ = the calibration coefficient
DN = the original luminance gray value
$offset$ = the absolute calibration coefficient offset

Step 3. Atmospheric correction: It is the process of eliminating the radiation errors caused by atmospheric scattering, absorption, and reflection, so as to obtain the true reflectivity of surface objects. Here, the fast line-of-sight atmospheric analysis of spectral hypercubes (FLAASH) atmospheric correction is used for the GF-1 reference data. It has been commercially applied and is one of the more accurate atmospheric correction models available. It is an atmospheric correction algorithm based on principal component analysis and uses the procedure of MODTRAN 4+ radiative transfer model (Wang et al., 2013) for pixel-based correction, which can eliminate or reduce the cascading effects caused by diffuse reflections and adjust the spectral smoothing caused by artificial suppression (Hao et al., 2008). Its spectral radiation equation is as follows:

$$L = (\frac{A\rho}{1-\rho_e S}) + (\frac{B\rho}{1-\rho_e S}) + L_\alpha \quad (2)$$

where L = the radiance of the pixel
A, B = the coefficients depending on the atmospheric and geometric conditions
ρ = the surface reflectance of the pixel
ρ_e = the average surface reflectance of the pixel and its surrounding area
S = the atmospheric albedo
L_α = the atmospheric backward scattered radiation

The GF-2 data are processed using the Quick Atmospheric Correction (QUAC) tool in ENVI to balance the processing time, result accuracy, and ease of batch processing. Compared with the FLAASH correction algorithm, the QUAC algorithm can make full use of remote sensing images to obtain spectral information of different ground objects, and perform fast and accurate atmospheric correction through empirical values to obtain the real surface reflectance without complex environmental parameters.

Step 4. Calculation of NDVI: After the above absolute radiation normalization, the reflectance data of GF-1 and GF-2 are obtained. The red light band and the near-infrared band are used for combined operation. The reference NDVI data were calculated from the reflectance data of GF-1, and the NDVI data to be normalized is calculated from GF-2 reflectance data. The calculation formula is as follows:

$$NDVI = \frac{\rho_{NIR} - \rho_{RED}}{\rho_{NIR} + \rho_{RED}} \quad (3)$$

where ρ_{NIR} = the near-infrared band
ρ_{RED} = the red band

Step 5. Prepare auxiliary data: Classification data and cloud mask data. The Classification data corresponding to the data to be normalized is obtained by applying ENVI IsoData Classification to GF-2 reflectance data. And deep learning-based cloud detection method named multi-scale convolutional feature fusion (MSCFF) (Li et al., 2019) is applied to obtain cloud mask data corresponding to the data to be normalized.

2.3 Methods

The SGloLM has a significant problem of mosaic seams when NDVI normalization is performed on multi-scene high-resolution images. Therefore, this study has improved it in two aspects. On the one hand, the coefficient solution of the SGloLM algorithm is improved. On the other hand, the MVC method is added.

2.3.1 Single-scene global linear model: Linear models are the most widely used typical models for cross-sensor NDVI conversion. In the earlier reference-based normalization, the global linear model is often applied to the normalization of reflectance data. Based on previous studies (Miura et al., 2013; Potapov et al., 2020; Gan et al., 2014), it can be found that there is usually a linear correlation between different sensors and multi-temporal images of the same region. In other words, their grayscale values in the same band can be interconverted by a linear equation. Therefore, the SGloLM method assumes that the relationship between the data to be normalized and the reference data can be described by a simple linear regression equation as:

$$y = a \cdot x + b \quad (4)$$

where x = the reflectance value of the experimental image
y = the normalized reflectance value of the experimental image
a, b = the slope and intercept of the linear regression equation

Based on the above assumptions, after downsampling the high-resolution data to be normalized to the resolution of the medium-resolution reference data, the slope and the intercept of the linear regression equation are solved according to the medium-resolution sample point pairs. And then the normalization results of each image element of the data to be normalized are calculated by this linear relationship element by element. The specific processing flow is as follows:

Step 1. The high-resolution data to be normalized should be downsampled to the medium resolution of the reference data.

Step 2. The purity of each medium resolution pixel is calculated according to the high-resolution classification data (6-10 categories). Then, through a given threshold (0.5-0.6), the pure pixel is determined. The calculation formula for pixel purity is as follows:

$$r = \frac{k_c}{m \times m} \quad (5)$$

where r = pixel purity
k_c = the number of pixels belonging to the feature category c, which has the largest proportion in any medium resolution pixel range
m = the scale ratio between the high-resolution and the medium-resolution

Step 3. Based on the pure pixels, the linear relational coefficients are solved by Huber-type M-estimation according to the following equation:

$$y_n = a \times x_n + b \tag{6}$$

where x_n = the downsampled data to be normalized
y_n = the corresponding medium-resolution reference data
a, b = the coefficients of the linear relationship

Errors in geometric correction, resampling, and unsupervised classification are bound to bring noise and outliers. However, the standard least-squares method is easily affected by these noises and outliers, which leads to errors in coefficient solving. Therefore, a more robust Huber type M-estimation is used here:

$$e_{uv} = a \times x_{uv} + b - y_{uv} \tag{7}$$

The coefficient is solved by minimizing $\sum_{uv} \rho(e_{uv})$, where ρ is the influence function. There are many influence functions in the robust estimation, and the Huber type influence function is selected here:

$$\rho(e_{uv}) = \begin{cases} \frac{e_{uv}^2}{2}, & |e_{uv}| \le c, \\ c|e_{uv}| - \frac{c^2}{2}, & |e_{uv}| > c \end{cases} \tag{8}$$

where c = the Huber parameter

In order to facilitate the optimization of the calculation process, the minimization problem of the following equation (9) can be equivalently transformed into the iterative reweighted least-squares problem:

$$\min \sum (w(e_{uv}) e_{uv})^2 \tag{9}$$

$w(e_{uv})$ is the weight of each pixel, equal to $\frac{\rho'(e_{uv})}{e_{uv}}$. In this way, coefficients can be solved by an iterative process.

Step 4. Each pixel of the data to be normalized is substituted into the linear relationship equation obtained above to obtain its normalized value. The calculation formula is as follows:

$$y'_m = a \times x_m + b \tag{10}$$

where x_m = the high-resolution data to be normalized
y'_m = the corresponding normalized value
a, b = the coefficients of the linear relationship obtained in step 3

2.3.2 Multi-scene global linear model: To address the problem of obvious multi-scene image mosaic seams that occurs when the SGloLM method is applied to product production. Based on the SGloLM method, this study proposes MGloLM. The improvements are made to alleviate the problem of obvious mosaic seams in a wide range of products. The improvement idea is as follows: when processing the data to be normalized in one scene, read in the adjacent image data of the top, bottom, left, and right four scenes at the same time, and carry out steps 1 and 2 in the previous subsection to obtain the pure pixels of each scene. And then solve the coefficients of the linear relationship equation based on the pure pixels of these five scenes to obtain the linear relationship equation. Finally, substitute each pixel of the data to be normalized is substituted into the linear relationship equation derived above to obtain its normalized value.

2.3.3 Maximum Value Composite method: The MVC can effectively reduce the effects of atmospheric aerosols, cloud shadows, and solar altitude angle, and has been widely used in the production of low and medium-resolution remote sensing vegetation index products (such as MOD13 and MYD13 based on EOS/MODIS sensors; PAL, GIMMS, and GVI based on AVHRR sensors; VGT-S10 based on VEGETATION sensors (Ge, 2016)). In this study, the NDVI data of one season was used as the basis to obtain the quarterly maximum NDVI using the MVC, which characterizes the best condition of vegetation growth in the current season. The calculation formula is as follows:

$$NDVI_{\max} = \max(NDVI_1, NDVI_2) \tag{11}$$

where $NDVI_{\max}$ = the maximum value of NDVI
$NDVI_1$, $NDVI_2$ = multiple NDVI values in different periods of the quarter

2.3.4 Precision evaluation: For the experimental results of this study, the reference data resampled to high-resolution was used as the standard data, and the accuracy was evaluated by qualitative and quantitative methods. The qualitative evaluation mainly includes the visual effect of the image and the comparison of its histogram. The quantitative evaluation is mainly completed by the following three indicators:

① The Correlation Coefficient (CC), the calculation formula is as follows:

$$r = \frac{\sum_i (\hat{y}_i - \bar{\hat{y}})(y_i - \bar{y})}{\sqrt{\sum_i (\hat{y}_i - \bar{\hat{y}})^2 \sum_i (y_i - \bar{y})^2}} \tag{12}$$

where r = the correlation coefficient
$\hat{y}_i$ = the value of the i th pixel of the normalized image
$\bar{\hat{y}}$ = the average value of the normalized image
y_i = the value of the i th pixel of the standard data
$\bar{y}$ = the mean value of the standard data

② The Mean Absolute Difference (MAD), the calculation formula is as follows:

$$MAD = \frac{1}{n}\sum_{i=1}^{n}|\hat{y}_i - y_i| \quad (13)$$

where MAD = the mean absolute error value
n = the number of pixels
$\hat{y}_i$ = the value of the i th pixel of the normalized image
y_i = the value of the i th pixel of the standard data

③ The Root Mean Squared Error (RMSE), the calculation formula is as follows:

$$RMSE = \sqrt{\frac{1}{n}\sum_{i=1}^{n}(\hat{y}_i - y_i)^2} \quad (14)$$

where $RMSE$ = the root mean square error
n = the number of pixels
$\hat{y}_i$ = the value of the i th pixel of the normalized image
y_i = the value of the i th pixel of the standard data

3. RESULTS AND ANALYSIS

In this study, two scenes of images were selected, normalization experiments were performed, and their normalization results were mosaicked, as well as qualitative and quantitative evaluations.

The experimental results are shown in Figure 3 below. Visually, the spatial pattern and spatial distribution of the images changed to a certain extent after normalization, with the SGloLM method showing the worst results, the normalized images of the SGloLM+MVC method being the most similar to the standard data used for evaluation. The mosaic seams of the SGloLM+MVC and the MGloLM+MVC methods are not obvious, and the improved SGloLM+MVC method can better eliminate the mosaic seams.

The histogram of experimental results of different methods in the small area at the lower right corner of Figure 3 is shown in Figure 4 below (the NDVI shown here is enlarged by 10,000 times). It can be seen from the figure that the histogram of normalized results is closer to the histogram of standard data than before normalization. Among them, the histogram curves of SGloLM +MVC and MGloLM +MVC methods are closest to the standard data.

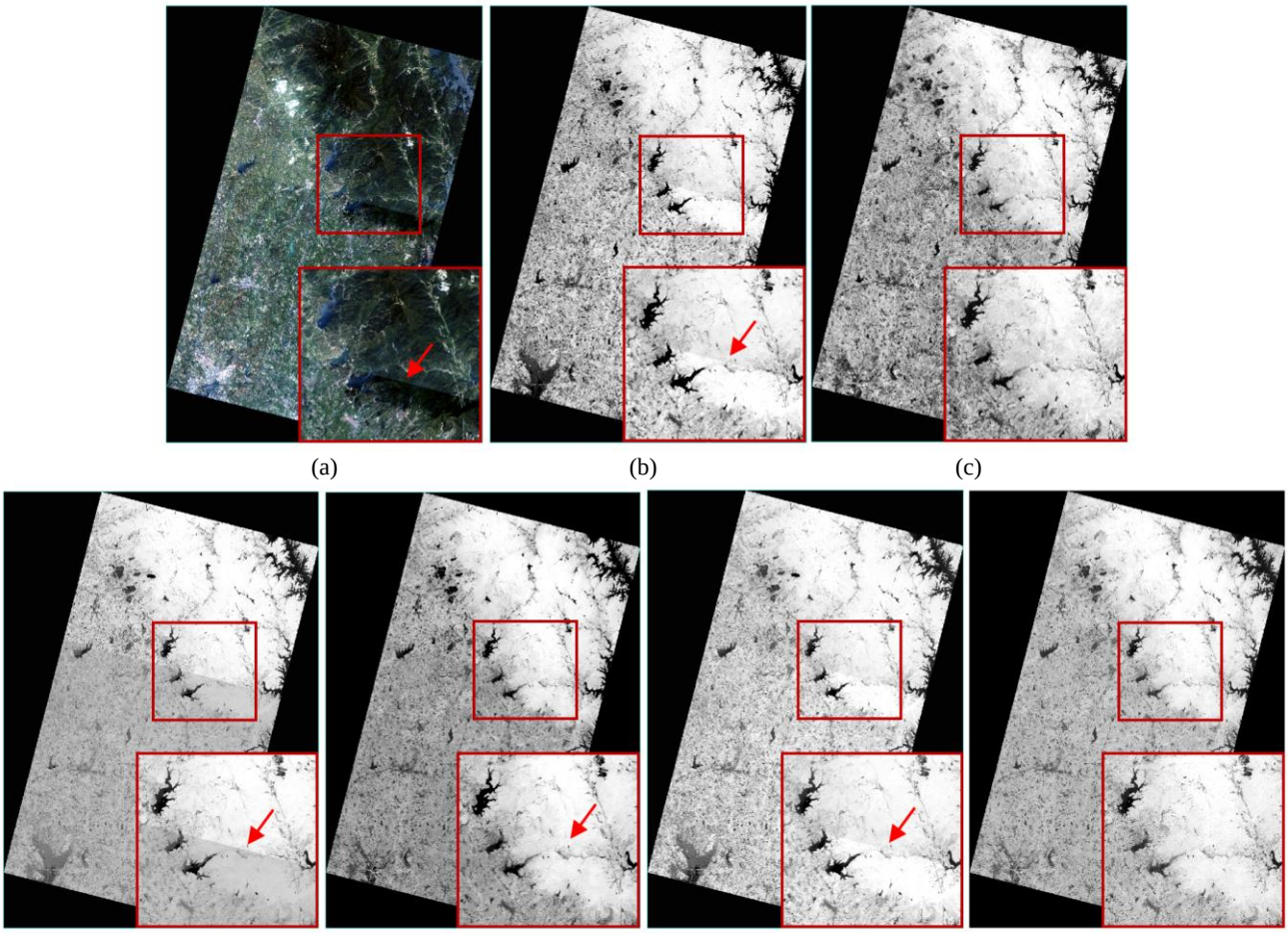

Figure 3. (a) Reflectance data before normalization, (b) NDVI data before normalization, (c) standard NDVI data, (d) NDVI data after SGloLM normalization, (e) NDVI data after SGloLM+MVC normalization, (f) NDVI data after MGloLM normalization, (g) NDVI data after MGloLM+MVC normalization NDVI data.

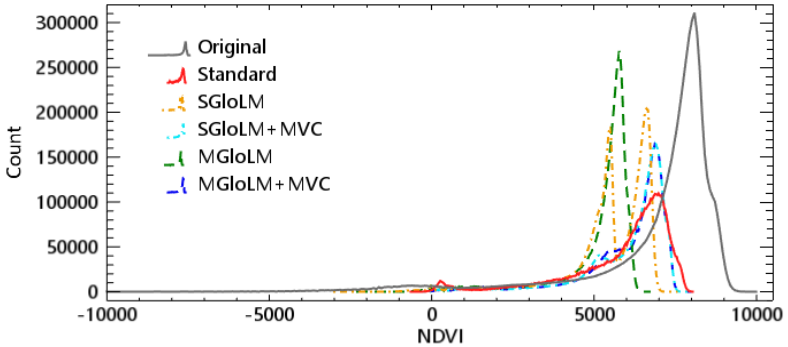

Figure 4. Comparison of histograms before and after normalization.

The quantitative evaluation results for this small area are shown in Table 2. Compared with the data before normalization, the normalized data of the three methods are better in all indicators. CC improves from 0.6852 to about 0.74, MAD decreases from 0.1598 to about 0.08, and RMSE decreases from 0.1965 to about 0.11. Among them, the SGloLM+MVC method has the largest CC, followed by MGloLM +MVC, the SGloLM+MVC method has the smallest MAD and RMSE, followed by MGloLM+MVC. Combining the three indicators, the SGloLM+MVC method has the best quantitative results, followed by MGloLM +MVC method, and the MGloLM method is the worst.

Evaluation Indicators	Before normalization	After normalization			
		SGloLM	SGloLM+MVC	MGloLM	MGloLM+MVC
CC	0.6852	0.7231	0.7804	0.6872	0.7682
MAD	0.1598	0.0855	0.0643	0.1117	0.0659
RMSE	0.1965	0.1150	0.1012	0.1345	0.1035

Table 2. Quantitative evaluation of normalized results.

4. CONCLUSION

In this study, using GF-1 WFV and GF-2 PMS multispectral data, combined with absolute radiometric correction and relative radiometric correction, the NDVI normalization method was studied. First, a series of pre-processing of the data was performed to obtain the reflectance data. Then, based on the reflectance data, relative radiation normalization was performed and the existing SGloLM method is improved to accommodate the production of high-resolution vegetation index data products on a large scale. The improvement mainly starts from two aspects. On the one hand, it is to improve the coefficient solution of the SGloLM method, using the data to be normalized and its adjacent images to jointly participate in the solution of the coefficients of the linear regression equation, and MGloLM is proposed. On the other hand, it is to add the MVC method, the maximum value of NDVI at different times in a season is synthesized to represent the best condition of vegetation growth in the current season. For the improved method, combined experiments were performed and qualitative and quantitative evaluations were done respectively. The experimental results show that visually, both SGloLM+MVC and MGloLM+MVC are more effective, and the SGloLM+MVC method is the best in terms of quantitative indicators.

REFERENCES

China High-resolution Earth Observation System (CHEOS) grid platform. https://www.cheosgrid.org.cn/.

Gan, W., Shen, H., Zhang, L., Gong, W., 2014. Normalization of NDVI from Different Sensor System using MODIS Products as Reference. IOP Conference Series: Earth and Environmental Science 17.

Gan, W., 2015. Research about the normalization of multi-source NDVI. Wuhan University.

Ge M., 2016. An Algorithm Study on Normalization of Vegetation Index based on Multi-source Remote Sensing Data. Chongqing University of Posts and Telecommunications.

Guo N., 2003. Vegetation Index and Its Advances. Arid Meteorology, 71-75.

Hao J., Yang W., Li Y., Hao J., 2008. Atmospheric Correction of Multi-spectral Imagery ASTER., Remote Sensing Information, 78-81.

Li, Z., Shen, H., Cheng, Q., Liu, Y., You, S., He, Z., 2019. Deep learning based cloud detection for medium and high resolution remote sensing images of different sensors. ISPRS Journal of Photogrammetry and Remote Sensing 150.

Miura, T., Turner, J.P., Huete, A.R., 2013. Spectral Compatibility of the NDVI Across VIIRS, MODIS, and AVHRR: An Analysis of Atmospheric Effects Using EO-1 Hyperion. Geoscience and Remote Sensing, IEEE Transactions on 51, p.1349-1359.

Potapov, P., Hansen, M.C., Kommareddy, I., Kommareddy, A., Turubanova, S., Pickens, A., Adusei, B., Tyukavina, A., Ying, Q., 2020. Landsat Analysis Ready Data for Global Land Cover and Land Cover Change Mapping.

Wang J., Ye Q., Lin Y., 2013. Comparing Effects of Different Atmospheric Correction Algorithms in Remote Sensing Dynamic Monitoring of Cyano Bacteria Bloom in Inland Lakes. Remote Sensing Technology and Application 28, 157-165.

Wu Y., 2014. The successful launch of the "GF-2" satellite, the newspaper interviewed experts related to the special project of Gaofen--Hotspot interpretation - Dialogue: My country's remote sensing satellites have entered the sub-meter "Gaofen era". http://cpc.people.com.cn/n/2014/0820/c83083-25501524.html.

Xu Y., 2019. Study on Surface Reflectance Normalization based on Multi-source medium-to-high Resolution Remote Sensing Data. Henan Polytechnic University.

Zhang X., 2009. Introduction of Several Vegetation Indices Based on EOS/MODIS. Journal of Anhui Agricultural Sciences 37, 12842-12845+12850.

Zhuo N., 2017. Research on the Object-oriented Method of City Features Extraction with GF-2 Remote-sensing Imagery. China University of Geosciences (Beijing).